


# Structural-Based Virtual Screening of FDA-Approved Drugs Repository for NSP16 Inhibitors, Essential for SARS-CoV-2 Invasion Into Host Cells: Elucidation From MM/PBSA Calculation

Bioinformatics and Biology Insights  
Volume 17: 1–9  
© The Author(s) 2023  
Article reuse guidelines:  
sagepub.com/journals-permissions  
DOI: 10.1177/11779322231171777  


Subodh Kumar<sup>1,2</sup>, Harvinder Singh<sup>1\*</sup>, Manisha Prajapat<sup>1\*</sup>, Phulen Sarma<sup>1,3\*</sup>, Anusuya Bhattacharyya<sup>4</sup>, Hardeep Kaur<sup>1</sup>, Gurjeet Kaur<sup>1</sup>, Nishant Shekhar<sup>1</sup>, Karanveer Kaushal<sup>5</sup>, Kalpna Kumari<sup>6</sup>, Seema Bansal<sup>1</sup>, Saniya Mahendiratta<sup>1</sup>, Arushi Chauhan<sup>7</sup>, Ashutosh Singh<sup>1</sup>, Rahul Soloman Singh<sup>1</sup>, Saurabh Sharma<sup>1</sup>, Prasad Thota<sup>8</sup>, Pramod Avti<sup>7</sup>, Ajay Prakash<sup>1</sup>, Anurag Kuhad<sup>2</sup> and Bikash Medhi<sup>1</sup>

<sup>1</sup>Department of Pharmacology, Postgraduate Institute of Medical Education and Research (PGIMER), Chandigarh, Chandigarh, India. <sup>2</sup>University Institute of Pharmaceutical Sciences (UIPS), Panjab University, Chandigarh, India. <sup>3</sup>Department of Pharmacology, All India Institute of Medical Sciences (AIIMS), Guwahati, Guwahati, India. <sup>4</sup>Department of Ophthalmology, Government Medical College & Hospital, Sector 32 (GMCH-32), Chandigarh, India. <sup>5</sup>Department of Ophthalmology, School of Medicine, Stanford University, Stanford, CA, USA. <sup>6</sup>Department of Anaesthesia, Postgraduate Institute of Medical Education and Research (PGIMER), Chandigarh, Chandigarh, India. <sup>7</sup>Department of Biophysics, Postgraduate Institute of Medical Education and Research (PGIMER), Chandigarh, Chandigarh, India. <sup>8</sup>Indian Pharmacopoeia Commission, Ghaziabad, India.

**ABSTRACT:** NSP16 is one of the structural proteins of the severe acute respiratory syndrome coronavirus-2 (SARS-CoV-2) necessary for its entrance to the host cells. It exhibits 2′O-methyl-transferase (2′O-MTase) activity of NSP16 using methyl group from S-adenosyl methionine (SAM) by methylating the 5-end of virally encoded mRNAs and shields viral RNA, and also controls its replication as well as infection. In the present study, we used in silico approaches of drug repurposing to target and inhibit the SAM binding site in NSP16 using Food and Drug Administration (FDA)-approved small molecules set from Drug Bank database. Among the 2456 FDA-approved molecules, framycetin, paromomycin, and amikacin were found to be significant binders against the SAM binding cryptic pocket of NSP16 with docking score of −13.708, −14.997 and −15.841 kcal/mol, respectively. Classical molecular dynamics (MD) simulation and molecular mechanics Poisson–Boltzmann surface area (MM/PBSA)-based binding free energy calculation depicted that all these three framycetin, paromomycin, and amikacin might be promising therapeutic leads towards SARS-CoV-2 infections via host immune escape inhibition pathway.

**KEYWORDS:** NSP16 (2′O-methyl-transferase), SARS-CoV-2, structure-based virtual screening, drug repurposing, MM/PBSA

**RECEIVED:** August 30, 2022. **ACCEPTED:** April 7, 2023.

**TYPE:** Original Research Article

**FUNDING:** The author(s) received no financial support for the research, authorship, and/or publication of this article.

**DECLARATION OF CONFLICTING INTERESTS:** The author(s) declared no potential conflicts of interest with respect to the research, authorship, and/or publication of this article.

**CORRESPONDING AUTHOR:** Bikash Medhi, Department of Pharmacology, Postgraduate Institute of Medical Education and Research (PGIMER), Chandigarh, Chandigarh 160012, India. Email: drbikashus@yahoo.com

## Introduction

The recent pandemic caused by severe acute respiratory syndrome coronavirus-2 (SARS-CoV-2) has imposed great threat to human kind.<sup>1</sup> Owing to the high infectivity and death rate, many attempts were made to identify suitable inhibitors against SARS-CoV-2. Some of the potential drug candidates proposed<sup>2</sup> and evaluated so far included chloroquine and hydroxychloroquine,<sup>3–6</sup> lopinavir/ritonavir,<sup>7–9</sup> cobicistat, darunavir,<sup>10</sup> tocilizumab,<sup>11–14</sup> remdesivir,<sup>9,15,16</sup> ivermectin, niclosamide, ribavirin, metformin, etc.<sup>2</sup> Among these tocilizumab, remdesivir, baricitinib were approved by Food and Drug Administration

(FDA).<sup>2</sup> However, most other drugs evaluated either failed in clinical trials or showed uncertain efficacy,<sup>17,18</sup> eg, hydroxychloroquine,<sup>6</sup> lopinavir/ritonavir,<sup>7</sup> metformin,<sup>2</sup> ivermectin.<sup>2</sup>

Coronavirus are enveloped positive-sensed RNA viruses.<sup>19</sup> The non-structural proteins of SARS-CoV-2 (NSP1–NSP16) play an important role in the entrance and replication of the virus in the host cell. Among the all NSPs, NSP16 possesses 2′O-methyl-transferase (2′O-MTase) activity.<sup>19</sup> S-adenosyl methionine (SAM) binds to NSP16 as a cofactor and plays important role in the methylation of 5′-end of virally encoded mRNAs. This methylation is crucial for RNA cap formation; an essential process for viral RNA stability and thus important for replication, infection, and is a crucial step to escape from host immune recognition.<sup>20–30</sup> Studies have shown that inhibiting or

\* Equal contribution, so designated as combined second author.



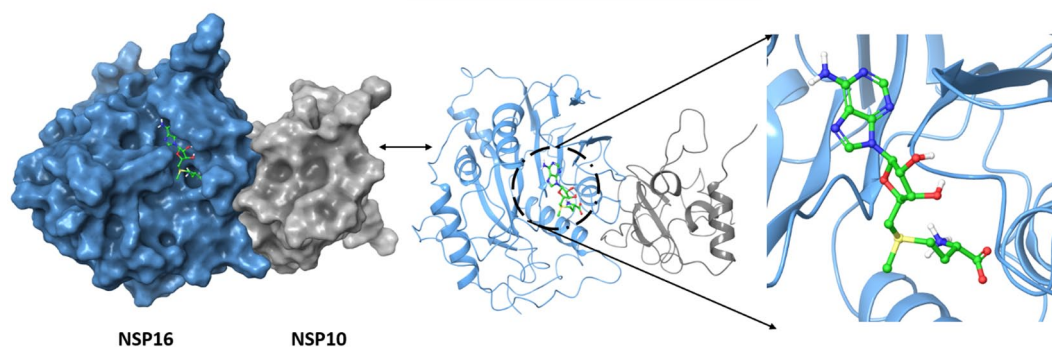


**Figure 1.** SAM ligand binding site in NSP16-NSP10 hetero dimer complex: here presenting surface image (A) and secondary image (B) of protein complex in which grey colour presenting NSP10, blue colour presenting NSP16, and red colour presenting SAM ligand located in binding pocket of NSP16. NSP indicates non-structural proteins; SAM, S-adenosyl methionine.

knocking out methylation activity relentlessly attenuated SARS-Cov-2 replication and infection.<sup>31</sup> Thus, NSP16 represents an important target for development of drugs against COVID-19.

The SAM binding site is already used by two studies from drug design perspective against COVID-19. In the first study by Tazikeh-Lemeski et al,<sup>32</sup> the authors have used a drug shape-based screen against a known template drug sinefungin (methyl transferase inhibitor). In the second study by Kumar et al,<sup>33</sup> the authors have evaluated natural compounds. In contrast to these two studies, our study uses a different approach for selection of leads. We screened all the FDA-approved drugs ( $n=2456$  drugs) for their binding affinity against the SAM binding pocket of NSP16 and optimal candidates were selected on the basis of docking score for their binding affinity towards the SAM binding site.

## Materials and Methods

For the current in silico studies, Dell precision tower desktop was used having LINUX Ubuntu OS 18.04.02 LTS, whereas Schrodinger Maestro version 2019-3 was used for docking and molecular dynamics (MD) simulation studies.

### Retrieval and preparation of ligands

For the screening purpose, we selected the small set of molecules (FDA-approved) from the Drug Bank database up to 10 January 2020 ( $n=2456$  drugs).<sup>34</sup> The Drug Bank database contains a comprehensive database of approved small molecules, large molecules, biological molecules, nutraceuticals, and experimental drugs as well as drug targets, and is freely accessible. Spatial data files (SDFs) of these 2456 approved molecules were obtained and prepared by means of ligprep module using default parameters, ie, OPLS3e forcefield at pH  $7.0 \pm 2.0$  using Epik for ionization protocol, tautomer generated, and specified chirality were retained during computations.<sup>35</sup> Ligand preparation is a crucial stage for further docking purposes and for the best low-energy isomers production, energy was minimized.<sup>35</sup>

### Selection of target PDB structure

In our study, we used NSP16 as the key target and our aim was to identify agents which competitively bind to the SAM binding pocket present in the NSP16–NSP10 hetero dimer complex and thus act as a competitive inhibitor of SAM binding and inhibit its 2'O-MTase activity. We selected an NSP16–NSP10 complex bound to SAM (PDB i.d. 6W4H, structure generated by X-ray diffraction) from the RCSB database, with a resolution of 1.80 Å with 0% side chain outliers and 0% Ramachandran outliers.<sup>36,37</sup>

### Protein preparation

For docking purposes, protein preparation was executed by means of the 'protein preparation wizard' tool of 'Maestro' and the energy was minimized.<sup>38-41</sup> To avoid the interference in binding pocket, water molecules outside 5.0 Å were excluded.

### Determination of the NSP16 binding pocket and grid generation

In eukaryotic cells, ribose 2'O-methyltransferases (2'O-MTases) catalyse the methylation process for the Cap-1 and sometimes Cap-2 generation at the ribose 2'O position of the first RNA nucleotide using a methyl group donated to SAM. One molecule of SAM binding in the catalytic core of  $\beta 1$  and  $\beta 2$  strands of the Rossmann-like fold results in the formation of a negatively charged SAM binding pocket in close proximity to the loops 6868–6876 and 6897–6905, and 6927–6945 (Figure 1). During the methyl group transfer in canonical SAM MTase motif, residues shows involvement are tetrad of Asp(6897,6912,6928,6931), Lys6968, Gly6871, Cys6913, Asn6899 and Glu7001.<sup>42</sup> In our study, we used SAM for the identification of the SAM binding cryptic pocket inside the NSP16–NSP10 hetero dimer complex (Figure 1).

### Grid generation

Receptor grid generation is a crucial step and using the Glide module of the Schrödinger tool gives us information about the

**Table 1.** Top 10 leads resulted from the virtual screening process with respective Glide docking scores.

S. NO.	DRUGBANK ID	NAME	GLIDE DOCKING SCORE
1	DB01421	Paromomycin	-15.841
2	DB00479	Amikacin	-14.997
3	DB00452	Framycetin	-13.708
4	DB00118	Ademetionine (also known as S-adenosyl methionine)	-13.006
5	DB03615	Ribostamycin	-12.953
6	DB09092	Xanthinol	-12.121
7	DB12615	Plazomicin	-11.306
8	DB00955	Netilmicin	-11.282
9	DB13274	Micronomicin	-11.246
10	DB13270	Dibekacin	-10.891

three-dimensional boundary generated for ligand–receptor binding at desired site.<sup>43</sup> In our study, the grid was generated against the SAM binding pocket site having the size of 10 Å and the coordinates  $x=99.89$ ,  $y=36.27$ ,  $z=16.75$  were used to employ virtual screening.

#### Virtual screening

‘Glide’ tool of ‘Maestro’ was used for the virtual screening experiment.<sup>43</sup> In our study, screening of a total of 2456 FDA-approved drugs was done in a tandem Hit Identification and Virtual Screening (HTVS) (50%), Standard precision (SP) (30%), and Extra precision (XP) (10%) progression.

#### Molecular dynamics

Ligands showing similar or better docking scores to SAM were further evaluated in molecular dynamics studies, whereas MD simulations of the NSP16–NSP10–drug complexes were evaluated using Desmond. Through the ‘system builder module’ of Schrödinger, initially, water model development was done followed by protein–ligand (P–L) complex neutralization, including sodium and chloride ions, and subsequently liquid simulations optimization was also minimized.<sup>39</sup> Once frame creations were done at 100 ps interval, the complexes were submitted for 200 ns simulations at number of particles ensemble (NPT) ensemble at 310 K, where N lay between 34900 and 35000 in the solvation box. Further C $\alpha$ -RMSD (Root Mean Square Deviation), side chains C $\alpha$ RMSF, ligand contact maps, as well as binding profile were obtained as a result of trajectory outputs.<sup>39</sup>

#### Binding free energy calculation

Binding free energy (BFE) is known as an evident parameter to predict complex stability in the manner of interaction energies. Ligands subjected to MD simulations were submitted for BFE calculation using *g\_mmpbsa* module.<sup>44</sup>

Molecular mechanics Poisson–Boltzmann surface area (MM-PBSA) combines the total three energetic terms, ie, potential energy (average molecular mechanics potential energy in a vacuum;  $E_{MM}$ ), solvation (energy of solvation;  $G_{solvation}$ ), and configurational entropy (contribution of entropy Temp. and S entropy) related to complex making in the gas phase.

$G_x = (E_{MM}) - TS + (G_{solvation})$ , where x is the ligand or the protein or P–L complex.

## Results

#### Virtual screening

In our study after grid generation, a virtual screening procedure was executed against target protein. The resulted top 10 ranked leads and their respective docking scores are shown in Table 1. The highest score of docking result was -15.841 for paromomycin and followed by amikacin (-14.997), framycetin (-13.708), and SAM (-13.708). Resulted docking scores were comparable with the standard or control (SAM). The threshold cut-off was set at the reference ligand SAM score (already known binder).

#### Classical molecular dynamics simulations

The virtual screening was followed by the classical molecular dynamics simulations that provide a more elaborative comparison in the mean of binding stability and interactions. Classical molecular dynamic simulations ran for the course of 200 ns of SAM (standard/reference) and the three lead ligands (paromomycin, amikacin, and framycetin) and protein complexes, which exhibited relatively better docking scores than SAM. Among paromomycin, framycetin, and amikacin, framycetin showed a lesser deviation in C $\alpha$ RMSD in comparison to SAM as shown in Figure 2. The stability of the P–L complex can be explained using the P–L interaction profile, which was dominated by the hydrogen bonds (H-bonds) interactions as shown in Figure 3A to D.

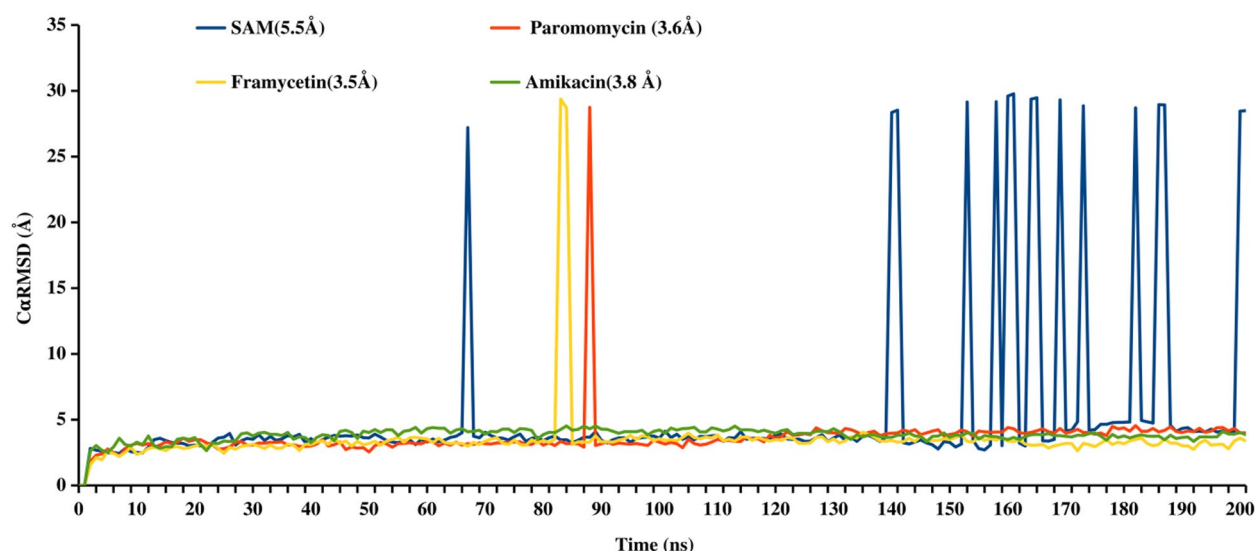


**Figure 2.** Line plot for detailed root mean square deviation for C-alpha of protein–protein complex in the presence of respective ligand subjected to the classical molecular dynamics (MD) simulation for 200ns (data presented as mean C $\alpha$ -RMSD(Å) for respective ligand). SAM, S-adenosyl methionine; RMSD, Root Mean Square Deviation.

The residues contributing to the stability and involved in P–L interactions in the context of all the ligands were H-bonds (yellow dashed line) Asp(6897, 6912, 6928, 6931), Lys6968, Gly6871, Cys6913. The H-bond interactions were followed by the salt bridges and ionic interaction involves Asp(6897, 6912, 6928, 6931) and Lys6968 (pink dashed line). Data showed in surface zoom in and zoom out in Figure 3A to C and P–L contacts in bar diagram S1 (Supplementary Figure 1).

### BFE calculations

For further validation of interaction profiles and stability of complexes, classical MD simulation trajectories were submitted for molecular mechanics Poisson–Boltzmann surface area (MM/PBSA)-based BFE calculation for every 1 ns time point frame of total of 200 trajectory frames. A total of four P–L complex MD simulation trajectories were submitted for BFE calculations resulted in the most negative average values for framycetin (−445.408 kJ/mol) and paromomycin (−405.719 kJ/mol), which indicates the stable complex formation as shown in Table 3. However, in case of SAM exhibited positive values for average BFE during the course of 200 ns MD simulations as shown in line plot of Figure 4.

### Discussion

Computational drug design methods (in silico) are useful in hypothesis generation and validation in drug discovery. These methods generally depend upon virtual affinity profiling and prediction. Thus, the in silico methods help us in prioritizing ligands for further testing. In an ideal setting, 100% predictions should be correct, however, this is not the case and the success probability is much lower. In the in vivo evaluation phase, many problems come, eg, bioavailability issues, toxicity, etc<sup>45</sup>. To avoid these, we have evaluated the

FDA-approved drugs, as the bioavailability of these drugs and toxicity profile is already known.<sup>4</sup> The SAM binding site is already used by many studies from drug design perspective against COVID-19. In the first study by Tazikeh-Lemeski et al,<sup>1</sup> the first screening was based on drug shape against a known template drug simefungin (MTase inhibitor) and compounds were selected on the basis of similarity score. They also evaluated four nucleoside analogues and one anti-inflammatory drug (Prednisolone). In the second study by Kumar et al,<sup>33</sup> the authors have evaluated natural compounds. Wishart<sup>34</sup> evaluated curcumin derivatives as inhibitors of NSP16. Similarly, other ligand databases evaluated were Nigerian medicinal plants,<sup>6</sup> natural inhibitors,<sup>7</sup> and SAM analogues,<sup>8</sup> etc. In contrast to these two studies, our study uses a different approach for selection of leads. For the screening purpose, we selected the database of FDA approved drugs from the Drug Bank database ( $n = 2456$  drugs).<sup>34</sup> The Drug Bank database contains a comprehensive database of approved small molecules, large molecules, biological molecules, nutraceuticals, and experimental drugs. Thus, the ligand databases are different from the previous studies. Again, we did a binding pocket-based screening, which is different from the methodology adopted by Tazikeh-Lemeski et al,<sup>32</sup> where they used a drug shape-based screening. Thus, the methodology of our study is different from already existing studies.

The importance of the SAM binding can be noted by the fact that inhibiting or knocking out methylation activity relentlessly attenuated SARS-Cov-2 replication and infection.<sup>9</sup>

In our study, we have used the SAM binding pocket on NSP16–NSP10 hetero dimer complex to identify potential molecules, which can compete with SAM for binding cleft and thus hamper the viral immune escape mechanisms of SARS-CoV-2. We selected 6W4H as a representative structure of

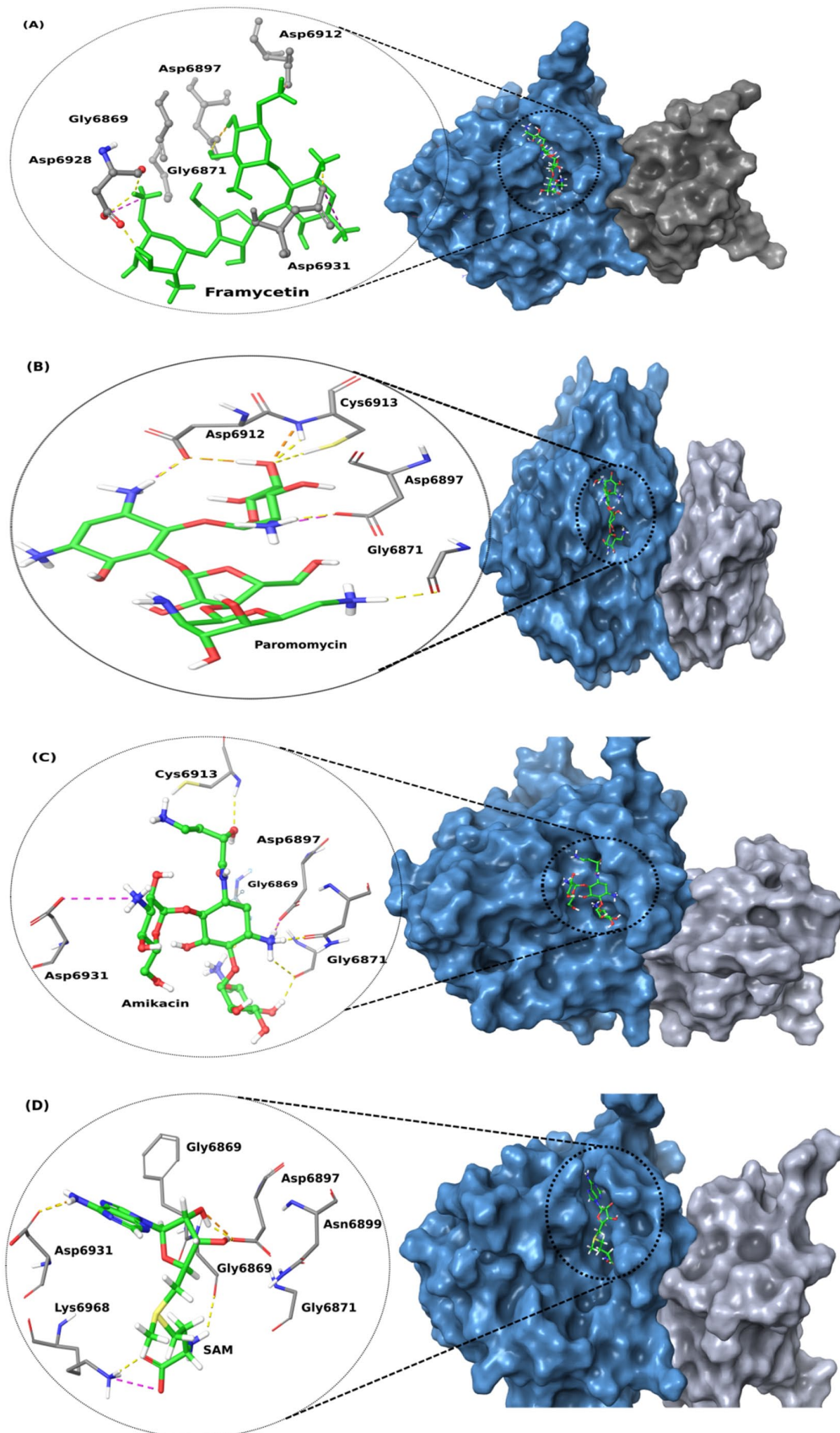


**Figure 3.** Protein–ligand interactions profile of (A) framycetin (B) paromomycin, (C) amikacin, and (D) SAM. Hydrogen bonds shown as yellow dashed line and salt bridges as pink dashed lined. Grey- and blue-coloured surface diagrams show NSP10 and NSP16, respectively. SAM indicates S-adenosyl methionine.

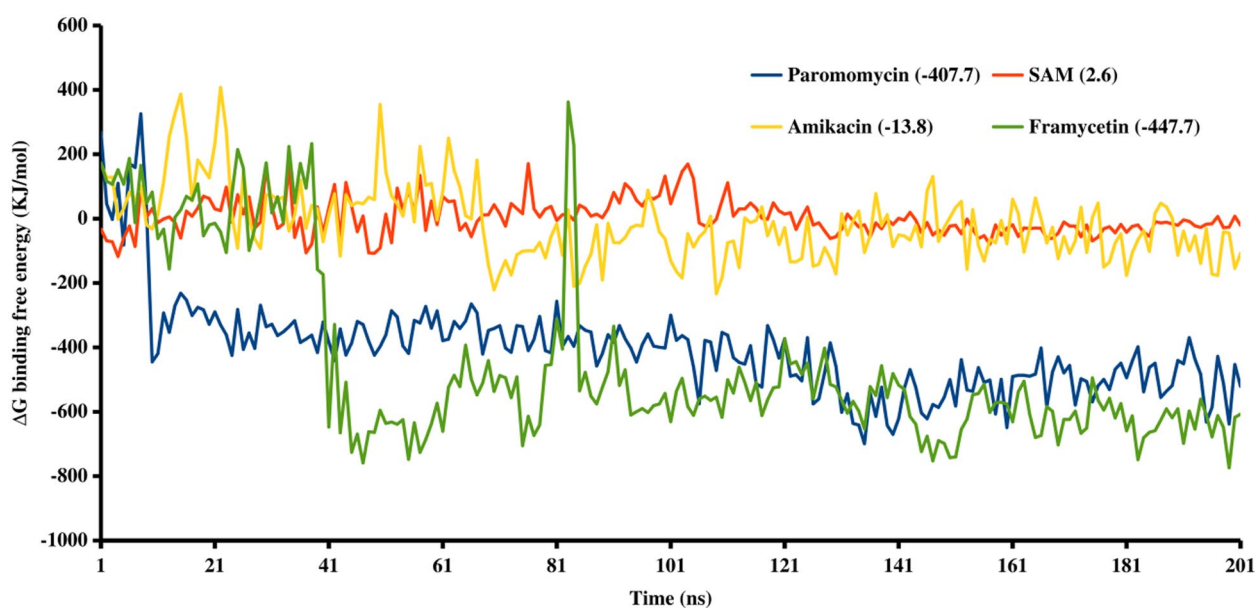


**Figure 4.** Line plot for negative binding free energy (using MM/PBSA) change during the long-run course of 200 ns classical MD simulation trajectory and respective mean binding free energy in kJ/mol. MM/PBSA indicates molecular mechanics Poisson–Boltzmann surface area; SAM, S-adenosyl methionine; MD, Molecular dynamics.

**Table 2.** Interaction profiles of selected ligands from molecular dynamics studies. .

NAME	CANONICAL SMILES	C $\alpha$ RMSD (Å)	AMINO ACID INTERACTION
Framycetin	<chem>C1C(C(C(C(C1N)OC2C(C(C(C(O2)CN)O)O)N)OC3C(C(C(O3)CO)OC4C(C(C(C(O4)CN)O)O)N)O)O)N</chem>	3.5	Asp(6897, 6912, 6928, 6931)
Paromomycin	<chem>C1C(C(C(C(C1N)OC2C(C(C(C(O2)CO)O)O)N)OC3C(C(C(O3)CO)OC4C(C(C(C(O4)CN)O)O)N)O)O)N</chem>	3.6	Asp6897, Asp6912, Cys6913
Amikacin	<chem>C1C(C(C(C(C1NC(=O)C(CCN)O)OC2C(C(C(C(O2)CO)O)N)O)O)OC3C(C(C(C(O3)CN)O)O)O)N</chem>	3.8	Gly6871, Asp6897, Cys6913, Asp6931
SAM	<chem>C[S+](CCC(C(=O)[O-])N)CC1C(C(C(O1)N2C=NC3=C(N=CN=C3)N)O)O</chem>	5.5	Gly6869, Asp6897, Asp6931, Lys6968.

Abbreviations: RMSD, Root Mean Square Deviation.

NSP16–NSP10 hetero dimer bound to SAM for the virtual screening. We generated the grid against the SAM binding site using 3D coordinates. On the basis of grid, a total of 2456 FDA-approved compounds library were screened in a tandem HTVS, SP, and XP progression. As a result of virtual screening, we identified 39 potential leads to the SAM binding site on NSP16, top 10 molecules are listed in Table 2 (Supplementary Table S1). Interestingly, SAM itself was identified as a potential binder (Table 2) in our virtual screening indicating the validity of our study results. Among all screened FDA-approved drugs library, top performing ligands were paromomycin, amikacin, and framycetin with a docking score of  $-15.841$ ,  $-14.997$ , and  $-13.708$ , respectively, which have better affinity than SAM.

To find potential binders, we ran classical molecular dynamics simulations of ligands with higher complex stability than SAM. In the molecular dynamics study also, these three ligands (framycetin, paromomycin, and amikacin)

resulted stable or less RMSD in complex formation. Binding affinity supported by the RMSD in the range of 3.5–5.5 Å and RMSF in the range of 0.8–1 Å (RMSF data not shown). All of the four ligands ranked using RMSD as framycetin (3.5 Å), paromomycin (3.6 Å), amikacin (3.8 Å), and SAM (5.5 Å). Stable complex formation is directly correlated with the decrease in RMSD supported by the non-covalent H-bond interactions and salt bridges. Maximal deviation peaks indicate the disassociation of NSP16–NSP10 within the defined periodic boundary, ie, box generation during the long course of classical MD simulation of 200 ns. So, the results suggested SAM has poor protein–protein (P–P) complex stability (Figure 2).

Framycetin interaction profile includes active binding site residues, ie, Asp6897, Asp6912, Asp6928, and Asp6931, and in H-bond interaction (dashed yellow line) as shown in the Figure 3A. Among these, Asp6912, Asp6928, and Asp6931 establish

**Table 3.** Negative binding free energy calculations for respective P–L complexes. Data presented as a mean and standard deviation in kJ/mol..

NAME	VAN DER WAAL ENERGY (kJ/mol)	ELECTROSTATIC ENERGY (kJ/mol)	POLAR SOLVATION ENERGY (kJ/mol)	SASA ENERGY (kJ/mol)	BINDING ENERGY (kJ/mol)
Framycetin	-10.666 +/- 1.227	-1189.572 +/- 46.186	761.699 +/- 30.446	-7.495 +/- 0.329	-445.408 +/- 19.209
Paromomycin	-25.560 +/- 1.419	-1087.154 +/- 21.065	716.778 +/- 16.990	-9.146 +/- 0.199	-405.719 +/- 10.986
Amikacin	-21.236 +/- 1.530	-307.291 +/- 20.066	319.522 +/- 16.729	-5.257 +/- 0.299	-13.427 +/- 8.027
SAM	-48.208 +/- 2.543	6.185 +/- 6.784	52.080 +/- 6.983	-7.245 +/- 0.360	2.510 +/- 3.772

Abbreviations: P–L, protein–ligand; SAM, S-adenosyl methionine; SASA, Solvent accessible surface area.

salt bridges (pink dashed line) played a pivotal role in the stability of the P–L complex formation.

Similarly, paromomycin interacted with the target site's active residues Asp6897, Asp6912, Cys6913, and Gly6871 through H-bonds (dashed yellow line), whereas salt bridges were formed by Asp6897, Asp6912 with the paromomycin (Figure 3B). A similar interaction pattern was found in the case of amikacin, which additionally interacts with Asp6931 through salt bridge formation as shown in Figure 3C. Whereas SAM interaction profile includes a little bit difference, ie, Lys6968, Gly6869 involved in the H-bond interaction (dashed yellow line), in addition to Asp6931 and Asp6897. There was a single salt bridge (dashed pink line) observed, which might be the reason behind poor stability and greater RMSD pattern (Figures 2 and 3D).

For further clarification of binding affinity towards SAM binding cleft MM/PBSA-based BFE calculation approach was employed. MM/PBSA-based BFE calculation is well-established approach and has significant prediction accuracy.<sup>44</sup> A similar trend was observed in BFE calculations as well as RMSD, listed in Table 3, and plotted in Figure 4. Most mean negative BFE values shown by framycetin (-445.4 kJ/mol), paromomycin (-405.7 kJ/mol), and amikacin (-13.4 kJ/mol). BFE calculation suggested that the framycetin, paromomycin, and amikacin have a greater affinity towards the binding site than the SAM that results in the positive BFE value 2.5 kJ/mol.

P–P complex disassociation was observed in the case of all leads except amikacin, which suggested the complex amikacin stabilized the P–P complex formation. This statement is supported by the BFE calculation as the most negative or at least negative BFE value shows greater stability than SAM that resulted in positive BFE and many P–P complex disassociations.

All the leads were belonging to aminoglycoside-derived antibiotics. First, framycetin, an antibiotic obtained from *Streptomyces lavendulae* (decaris) and specifically containing neomycin B, is used in bacterial eye infections. Framycetin exerts an antibacterial effect through binding with 16S rRNA and 30S-subunit protein, interfering with the translational machinery of the bacteria.<sup>46</sup> Due to the mechanism of action, it shows activity against aerobic bacteria only not towards viruses and fungi. However, our study results suggested that it might be a new mechanism of action of Framycetin against SARS-CoV-2, but preclinical experiments are required to support this hypothesis.

Second, paromomycin is derived from *Streptomyces rimosus* var. paromomycin, with amoebicidal, antibacterial, and anti-parasitic activities. Paromomycin has a similar mechanism of action as framycetin. It is also used as a therapeutic against visceral leishmaniasis. In 2006, paromomycin got approval for the treatment of the same caused by *Leishmania donovani*. Regarding antiviral activity, paromomycin–arginine conjugates also called aminoglycoside–arginine conjugates (AACs) exhibit anti-HIV-1 potential as well as numeral activities interrelated

to Tat antagonism apart from HIV-1 RNA binders. These AACs showed their potential as inhibitors to arrest the entry of viruses in to the host cells.<sup>46</sup> Regarding anti-SARS-CoV-2 activity, previous *In-Silico* studies have found that paromomycin binds against the S1 and main protease of SARS-CoV-2.<sup>47</sup>

Another semi-synthetic aminoglycoside antibiotic shown a comparable docking score is amikacin with SAM, which has a broad-spectrum antibacterial activity. Amikacin is effective against majority of the known strains that show resistance to other aminoglycosides. Amikacin formulation takes place through the acetylation of 1(-)- $\gamma$ -amino- $\alpha$ -hydroxybutyryl side chain at C-1 amino group of the deoxystreptamine moiety of kanamycin A. Although aminoglycosides have been used since the 1940s to treat bacterial infections but recently reported that some aminoglycosides, such as amikacin, have shown potential as antiviral activity against HIV as well as for the treatment of genetic disorders and are in clinical trials.<sup>48</sup> This viral inhibition was found to be through the expression of interferon (IFN)-stimulated genes (ISGs) in a TLR3-dependent manner. In our study, amikacin was found as a potential binder to the SAM binding site of NSP16 in SARS-CoV-2, these findings are supported by another study which revealed that certain aminoglycosides can inhibit virus replication *in vitro*.<sup>49</sup> The results suggest the consistency in the potential of amikacin against SARS-CoV-2 and are supported by an *in-vitro* study showing IC<sub>50</sub> of 16.81  $\mu$ M (NRC-03-nhCoV strain).<sup>50</sup> The use of framycetin is mostly limited as a topical preparation as it is poorly absorbed.<sup>51,52</sup> Despite showing an antiviral effect, this might be the reason of its limited use for surface infection only. Among the other leads which also showed the potential against SARS-CoV-2 with a top-ranked docking score in our *in silico* study, have been shown *in vitro* antiviral activity include ribostamycin, xanthinol, but there are no studies of these potential drugs against SARS-CoV-2.<sup>53,54</sup>

## Conclusion

In conclusion, framycetin, paromomycin, and amikacin were found to be significant binders against the SAM binding site of NSP16 in virtual screening and MD simulation studies. BFE calculations clarify the binding affinity trend as found in RMSD. Among these, amikacin has evidence of anti-coronavirus action *in vitro* highlighting the importance of our findings. This study opens the gateway for further *in vitro/in vivo* studies for framycetin and paromomycin.

## Limitations and Alternatives of the Study

*In-silico* approaches for drug repurposing to target and inhibit the SAM binding site have some drawbacks and disadvantages, including limited availability of data, limited knowledge of drug interactions and lack of experimental validation. So, the alternatives include high-throughput screening and rational drug design which can complement or replace *in silico* approaches to improve the efficiency and accuracy of drug discovery.

## Acknowledgements

Support of the Experimental Pharmacology Laboratory (EPL) team, Department of Pharmacology, PGIMER Chandigarh is highly acknowledged.

## Author Contributions

Subodh Kumar, Phulan Sarma, Pramod Avti, Anurag Kuhad, and Bikash Medhi contributed in designed, supervision, and execution of manuscript. Harvinder Singh, Manisha Prajapat, Anusuya Bhattacharyya, Hardeep Kaur, Gurjeet Kaur, Nishant Shekhar contributed in *In-Silico* experiments execution. Karanveer Kaushal, Kalpna Kumari, Seema Bansal, Saniya Mahendiratta, Arushi Chauhan, and Ashutosh Singh, Saurabh Sharma, and Prasad Thota contributed in manuscript writing and editing. Subodh Kumar, Phulen Sarma, and Ajay Prakash contributed in results and statistical analysis. All authors reviewed the manuscript.

## Abbreviations

Severe acute respiratory syndrome-coronavirus-2 (SARS-CoV-2); non-structural proteins 16 (NSP16); S-adenosyl methionine (SAM), binding free energy (BFE), protein-protein (P-P), protein-ligand (P-L)

## Ethical Approval and Consent to Participate

Not Applicable.

## Consent for Publication

Yes, the manuscript is submitted with the consent of all authors.

## Availability of Supporting Data

Yes.

## SUPPLEMENTAL MATERIAL

Supplemental material for this article is available online.

## REFERENCES

1. WHO Coronavirus (COVID-19) Dashboard. Accessed 25 September 2021. <https://covid19.who.int>
2. Aghamirza Moghim Aliabadi H, Eivazzadeh-Keihan R, Beig Parikhani A, et al. COVID-19: a systematic review and update on prevention, diagnosis, and treatment. *MedComm*. 2022;3:e115.
3. Ferner RE, Aronson JK. Chloroquine and hydroxychloroquine in covid-19. *BMJ*. 2020;369:m1432.
4. Aminoquinolines against coronavirus disease 2019 (COVID-19): chloroquine or hydroxychloroquine. Accessed 26 September 2021. <https://www.ncbi.nlm.nih.gov/pmc/articles/PMC7156117/>
5. Hydroxychloroquine: a potential ethical dilemma for rheumatologists during the COVID-19 pandemic. *J Rheumatol*. 2020;47:783-786. <https://www.jrheum.org/content/early/2020/04/01/jrheum.200369>
6. Sarma P, Kaur H, Kumar H, et al. Virological and clinical cure in COVID-19 patients treated with hydroxychloroquine: a systematic review and meta-analysis. *J Med Virol*. 2020;92:776-785.
7. Bhattacharyya A, Kumar S, Sarma P, et al. Safety and efficacy of lopinavir/ritonavir combination in COVID-19: a systematic review, meta-analysis, and meta-regression analysis. *Indian J Pharmacol*. 2020;52:313-323.
8. Arabi YM, Asiri AY, Assiri AM, et al. Treatment of Middle East respiratory syndrome with a combination of lopinavir/ritonavir and interferon- $\beta$ 1b (MIRACLE trial): statistical analysis plan for a recursive two-stage group sequential randomized controlled trial. *Trials*. 2020;21:8.
9. Cao B, Wang Y, Wen D, et al. A trial of Lopinavir-Ritonavir in adults hospitalized with severe Covid-19. *N Engl J Med*. 2020;382:1787-1799.



10. Pant S, Singh M, Ravichandiran V, Murty USN, Srivastava HK. Peptide-like and small-molecule inhibitors against Covid-19. *J Biomol Struct Dyn.* 2021;39:2904-2913.
11. Michot JM, Albiges L, Chaput N, et al. Tocilizumab, an anti-IL-6 receptor antibody, to treat COVID-19-related respiratory failure: a case report. *Ann Oncol.* 2020;31:961-964.
12. Bennardo F, Buffone C, Giudice A. New therapeutic opportunities for COVID-19 patients with Tocilizumab: possible correlation of interleukin-6 receptor inhibitors with osteonecrosis of the jaws. *Oral Oncol.* 2020;106:104659.
13. Luo P, Liu Y, Qiu L, Liu X, Liu D, Li J. Tocilizumab treatment in COVID-19: a single center experience. *J Med Virol.* 2020;92:814-818.
14. Zhang X, Song K, Tong F, et al. First case of COVID-19 in a patient with multiple myeloma successfully treated with tocilizumab. *Blood Adv.* 2020;4:1307-1310.
15. Remdesivir in the treatment of coronavirus disease 2019 (COVID-19): a simplified summary. Accessed 25 September, 2021. <https://www.ncbi.nlm.nih.gov/pmc/articles/PMC7256348/>
16. Elfiky AA. Ribavirin, Remdesivir, Sofosbuvir, Galidesivir, and Tenofovir against SARS-CoV-2 RNA dependent RNA polymerase (RdRp): a molecular docking study. *Life Sci.* 2020;253:117592.
17. Gold ER, Edwards AM. Overcoming market failures in pandemic drug discovery through open science: a Canadian solution. *Front Drug Dis.* 2022;2:898654. <https://www.frontiersin.org/articles/10.3389/fddsv.2022.898654>
18. Maziarz M, Stencel A. The failure of drug repurposing for COVID-19 as an effect of excessive hypothesis testing and weak mechanistic evidence. *Hist Philos Life Sci.* 2022;44:47.
19. Snijder EJ, Bredenbeek PJ, Dobbe JC, et al. Unique and conserved features of genome and proteome of SARS-coronavirus, an early split-off from the Coronavirus group 2 lineage. *J Mol Biol.* 2003;331:991-1004.
20. Züst R, Cervantes-Barragan L, Habjan M, et al. Ribose 2'-O-methylation provides a molecular signature for the distinction of self and non-self mRNA dependent on the RNA sensor Mda5. *Nat Immunol.* 2011;12:137-143.
21. Decroly E, Debarnot C, Ferron F, et al. Crystal structure and functional analysis of the SARS-coronavirus RNA cap 2'-O-methyltransferase nsp10/nsp16 complex. *PLoS Pathog.* 2011;7:e1002059.
22. In Vitro reconstitution of SARS-Coronavirus mRNA cap methylation. *PLoS Pathog.* 2010;6:e1000863. <https://journals.plos.org/plospathogens/article?id=10.1371/journal.ppat.1000863>
23. Decroly E, Imbert I, Coutard B, et al. Coronavirus nonstructural protein 16 is a cap-0 binding enzyme possessing (nucleoside-2'-O)-methyltransferase activity. *J Virol.* 2008;82:8071-8084.
24. Fehr AR, Perlman S. Coronaviruses: an overview of their replication and pathogenesis. *Coronaviruses.* 2015;1282:1-23.
25. Ke M, Chen Y, Wu A, et al. Short peptides derived from the interaction domain of SARS coronavirus nonstructural protein nsp10 can suppress the 2'-O-methyltransferase activity of nsp10/nsp16 complex. *Virus Res.* 2012;167:322-328.
26. Menachery VD, Gralinski LE, Mitchell HD, et al. Middle east respiratory syndrome coronavirus nonstructural protein 16 is necessary for interferon resistance and viral pathogenesis. *mSphere.* 2017;2:e00346.
27. Daffis S, Szretter KJ, Schriewer J, et al. 2'-O methylation of the viral mRNA cap evades host restriction by IFIT family members. *Nature.* 2010;468:452-456.
28. Chen Y, Su C, Ke M, et al. Biochemical and structural insights into the mechanisms of SARS coronavirus RNA ribose 2'-O-methylation by nsp16/nsp10 protein complex. *PLoS Pathog.* 2011;7:e1002294.
29. Menachery VD, Debbink K, Baric RS. Coronavirus non-structural protein 16: evasion, attenuation, and possible treatments. *Virus Res.* 2014;194:191-199.
30. Snijder EJ, Decroly E, Ziebuhr J. The nonstructural proteins directing coronavirus RNA synthesis and processing. *Adv Virus Res.* 2016;96:59-126.
31. Wu C, Liu Y, Yang Y, et al. Analysis of therapeutic targets for SARS-CoV-2 and discovery of potential drugs by computational methods. *Acta Pharm Sin B.* 2020;10:766-788.
32. Tazikheh-Lemeski E, Moradi S, Raoufi R, Shahlaei M, Janlou MAM, Zolghadri S. Targeting SARS-COV-2 non-structural protein 16: a virtual drug repurposing study. *J Biomol Struct Dyn.* 2021;39:4633-4646.
33. Kumar M, Roy A, Rawat RS, et al. Identification and structural studies of natural inhibitors against SARS-CoV-2 viral RNA methyltransferase (NSP16). *J Biomol Struct Dyn.* 2022;40:13965-13975.
34. Wishart DS, Feunang YD, Guo AC, et al. DrugBank 5.0: a major update to the DrugBank database for 2018. *Nucleic Acids Research.* 2018;46:D1074-1082.
35. LigPrep| Schrödinger. Accessed 6 September 2021. <https://www.schrodinger.com/products/ligprep>
36. Bank RPD. RCSB PDB – 6W4H: 1.80 angstrom resolution crystal structure of NSP16 – NSP10 complex from SARS-CoV-2. Accessed 6 September 2021. <https://www.rcsb.org/structure/6W4H>
37. Bank RPD. RCSB PDB. Accessed 4 April 2020. <http://www.rcsb.org/>
38. Maestro-Training Home and Schrödinger. Accessed 6 September 2021. <https://www.schrodinger.com/training/maestro11/home>
39. Desmond| Schrödinger. Accessed 27 March 2020. <https://www.schrodinger.com/desmond>
40. Sastry GM, Adzhigirey M, Day T, Annabhimoju R, Sherman W. Protein and ligand preparation: parameters, protocols, and influence on virtual screening enrichments. *J Comput Aided Mol Des.* 2013;27:221-234.
41. Molecular docking: a powerful approach for structure-based drug discovery. *Curr Comput Aided Drug Des.* 2011;7:146-517. <https://www.ncbi.nlm.nih.gov/pubmed/21534921>
42. Rosas-Lemus M, Minasov G, Shuvalova L, et al. The crystal structure of nsp10-nsp16 heterodimer from SARS-CoV-2 in complex with S-adenosylmethionine. *Biochemistry.* 2020. <http://biorxiv.org/lookup/doi/10.1101/2020.04.17.047498>. Accessed January 11, 2021.
43. Glide: Schrodinger. <https://www.schrodinger.com/products/glide>
44. Kumari R, Kumar R, Lynn A. G\_mmpbsa – A GROMACS tool for high-throughput MM-PBSA calculations. *J Chem Inf Model.* 2014;54:1951-1962.
45. Sacan A, Ekins S, Kortagere S. Applications and limitations of in silico models in drug discovery. *Methods Mol Biol.* 2012;910:87-124.
46. Borkow G, Vijayabaskar V, Lara HH, Kalinkovich A, Lapidot A. Structure-activity relationship of neomycin, paromomycin, and neamine-arginine conjugates, targeting HIV-1 gp120-CXCR4 binding step. *Antiviral Res.* 2003;60:181-192.
47. Tariq A, Mateen RM, Afzal MS, Saleem M. Paromomycin: a potential dual targeted drug effectively inhibits both spike (S1) and main protease of COVID-19. *Int J Infect Dis.* 2020;98:166-175.
48. Cohen JI. New activities for old antibiotics. *Nat Microbiol.* 2018;3:531-532.
49. Hermann T. Aminoglycoside antibiotics: old drugs and new therapeutic approaches. *Cell Mol Life Sci.* 2007;64:1841-1852.
50. Mostafa A, Kandeil A, Elshaher YAMM, et al. FDA-approved drugs with potent in vitro antiviral activity against severe acute respiratory syndrome Coronavirus 2. *Pharmaceuticals (Basel).* 2020;13:E443.
51. Horsburgh AG. Framycetin sulphate (Soframycin) as a pre-operative bowel-sterilizing agent. *Gut.* 1961;2:51-52.
52. Stidolph NE, Alston JM. The use of soframycin (framycetin sulphate) for intestinal sterilization. *Gut.* 1960;1:323-325.
53. Ennifar E, Paillart JC, Bodlenner A, et al. Targeting the dimerization initiation site of HIV-1 RNA with aminoglycosides: from crystal to cell. *Nucleic Acids Res.* 2006;34:2328-2339.
54. Kucherov II, Rytik PG, Podol'skaya IA, Mistryukova LO, Korjev MO. Novel inhibitors of HIV discovered among existing classes of pharmaceutical compounds indicated for unrelated clinical indications. *Curr Pharm Des.* 2009;15:1187-1190.